J. Biochem. 2012;151(1):89–97 doi:10.1093/jb/mvr126

JB THE JOURNAL OF BIOCHEMISTRY

Identification and biochemical characterization of a novel autotaxin isoform, ATXδ, with a four-amino acid deletion

Received August 4, 2011; accepted September 3, 2011; published online October 11, 2011

Takafumi Hashimoto[1], Shinichi Okudaira[1], Koji Igarashi[2], Kotaro Hama[1], Yutaka Yatomi[3] and Junken Aoki[1,4,*]

[1]Department of Molecular and Cellular Biochemistry, Graduate School of Pharmaceutical Science, Tohoku University, 6-3 Aoba Aramaki, Aoba-ku, Sendai, Miyagi 980-8578; [2]Bioscience Division, Reagent Development Department, AIA Research Group, TOSOH Corporation, Kanagawa 252-1123; [3]Department of Clinical Laboratory Medicine, Graduate School of Medicine, The University of Tokyo, 7-3-1 Hongo, Bunkyo-ku, Tokyo 113-8655; and [4]PRESTO, JST, 4-1-8 Honcho, Kawaguchi-shi, Saitama, 332-0012, Japan

*Junken Aoki. Department of Molecular and Cellular Biochemistry, Graduate School of Pharmaceutical Science, Tohoku University, 6 – 3 Aoba Aramaki, Aoba – ku, Sendai, Miyagi 980 – 8578, Japan. Tel: +81-22-795-6860, Fax: +81-22-795-6859, email: jaoki@mail.pharm.tohoku.ac.jp

Autotaxin (ATX) is lysophospholipase D, which converts lysophospholipids such as lysophosphatidylcholine (LPC) to lysophosphatidic acid (LPA), a bioactive lipid mediator with multiple biological roles. ATX is present in high concentrations in various biological fluids and is responsible for LPA production in these fluids. The plasma ATX level is altered in some pathophysiological conditions. Three splicing isoforms of ATX have been reported so far (ATXα, β and γ). In this study, we identified and characterized ATXδ, a novel alternative splice variant of ATX, which has a four-amino acid deletion in the L2 linker region of ATXβ. ATXδ was found to be the second major isoform following ATXβ and fully active. ATXβ and ATXδ showed similar divalent cation sensitivity and cell motility-stimulating activity. ATXβ and ATXδ are present in wide range of organism from fish to mammals. Among them, only ATXδ was found in *Gallus gallus* and *Xenopus laevis*, suggesting the indispensable role of the isoform. ATXδ was expressed in various human tissues with different expression patterns from that of ATXβ. These results show that ATXδ is a second major ATX isoform sharing similar biochemical characters with the major isoform, ATXβ, and is a potential biomarker.

Keywords: alternative splicing/autotoxin/lysophosphatidic acid/lysophosphatidylcholine/lysophospholipase D.

Abbreviations: ATX, autotoxin; LPA, lysophosphatidic acid; LPC, lysophosphatidylcholine; lysoPLD, lysophospholipase D; PDE, phosphodiesterase; *p*NP-TMP, *para*-nitrophenyl thymidine 5′-monophosphate.

Autotaxin (ATX, also known as NPP2 or ENPP2) is a secreted glycoprotein with a molecular weight of ~100 kDa. ATX was originally identified as a cancer cell motility-stimulating factor in conditioned media of a human melanoma cell line (*1*). ATX is now recognized as a major enzyme that produces lysophosphatidic acid (LPA). LPA is a lipid mediator that induces many kinds of cellular responses including cellular proliferation, prevention of apoptosis, cell migration, cytokine and chemokine secretion, platelet aggregation, smooth muscle contraction, transformation of smooth muscle cells and neurite retraction (*2*, *3*). Six G-protein-coupled receptors (GPCRs) specific to LPA have been identified and named LPA_{1-6}. It is likely that most of the LPA actions are mediated by these GPCRs. It has been shown that LPA has a variety of roles in both physiological and pathological conditions including brain development (*4*, *5*), embryo implantation (*6*, *7*), development of cancer (*3*), development of fibrosis (*8*, *9*) and lymphocyte trafficking (*10*). Because ATX knockout mice are embryonically lethal due to an abnormality of blood vessels (*11*, *12*), LPA is believed to have a critical role in embryonic vascular formation.

LPA is produced by either deacylation of phosphatidic acid (PA) mediated by phospholipase A_1/A_2 or polar head removal reaction of LPLs mediated by phospholipase D (*13*, *14*). The latter pathway is the major pathway, which mainly occurs in biological fluids such as plasma (*15*). There is accumulating evidence that ATX produces LPA by its lysophospholipase D (lysoPLD) activity (*11*, *12*, *16*, *17*). Indeed, the LPA level in human serum samples strongly correlates with the ATX level, and LPA production is completely absent in ATX-depleted serum (*11*, *17*). The ATX level in plasma or serum is altered in some pathophysiological conditions such as chronic liver diseases (*16*), obesity (*18*), cancer (*19*, *20*) and pregnancy (*21*). Thus, ATX may be a potential diagnostic marker of these diseases.

So far, three alternative splicing ATX isoforms have been identified: ATXα (ATXm), ATXβ (ATXt) and ATXγ (PD-Iα) that are produced by alternative splicing (*22*). The major isoform, ATXβ, does not have exons 12 and 21. ATXα was isolated from the conditioned media of a human melanoma cell line and has exon 12. ATXγ, which has exon 21, was identified in rat brain. All ATX isoforms have been shown to be enzymatically active. During the cloning of human ATXβ, we found that there is another ATX isoform, designated ATXδ that lacks four amino acids in the L2

linker region. In this article, we describe biochemical characteristics of a novel ATX isoform, ATXδ and compared it with other ATX isoforms.

Materials and Methods

Cloning of human ATX isoforms

Total RNAs from human tissues (kidney, brain and skeletal muscle) and human cancer cell lines (A2058 and SNB-78) were reverse-transcribed using oligo (dT) primers and SuperScript III (Invitrogen). cDNAs for ATXα, ATXβ, ATXγ, ATXδ and ATXε were amplified by nested PCR. Nested first PCR was performed using the cDNA prepared above as a template and two primers: 5′-GAACACGCTGCAAAAGGCTTTCC-3′ and 5′-CCAGTTGA TAAGACTGTACTGCAG-3′. Nested second PCR was performed using first PCR products as templates and two primers: 5′-ATTTAA ATCCACCATGGCAAGGAGGAGCTCGTTCC-3′ and 5′-GCG GTACCTTAAATCTCGCTCTCATATGTATGC-3′. The amplified cDNA was sub-cloned into SwaI/KpnI sites of pCALNL5 vector. Identification of cloned cDNA was performed by DNA sequencing by dideoxy method.

Recombinant ATX

HEK293 cells were cultured in Dulbecco's modified Eagle's medium (DMEM, SIGMA) supplemented with 10% fetal calf serum (FCS), antibiotics and L-glutamine. DNA transfection was performed using Lipofectamine 2000 Reagent (Invitrogen) according to the manufacture's protocol in serum-free OPTI-MEM medium. Forty-eight hour after transfection, culture supernatant was collected and used as an enzyme source.

Western blotting

Western blotting was performed as reported previously (*23*) after protein separation with 7.5% gel. Protein samples separated by sodium dodecyl sulfate–polyacrylamide gel electroporesis (SDS–PAGE) were transferred to nitrocellulose membranes. Anti-ATX monoclonal antibody 3D1 (1 : 200) was used as primary antibody and horseradish peroxidase-conjugated anti-rat immunoglobulin (1 : 2000) as a second antibody (American Qualex).

LysoPLD assay

LysoPLD activity of ATX was determined by measuring choline liberated from lysophosphatidylcholine (LPC, 2 mM) (*24*). Briefly, recombinant ATX was mixed with LPC (with 12 : 0, 14 : 0, 16 : 0, 18 : 0, 18 : 1, 18 : 2, 20 : 0), lyso platelet activating factor (lysoPAF), sphingocylphosphorylcholine (SPC) or egg phosphatidylcholine (PC) in assay buffer (100 mM Tris–HCl, 5 mM $MgCl_2$, 500 mM NaCl, 0.05% Triton X-100, pH 9.0) and incubated for 3 h at 37°C. Liberated choline was quantified using choline oxidase (*24*). The activity was indicated by the generation rate of choline per unit time and protein mass (pmol/ng/h).

Examination of ATX thermal stability

To determine thermal stability of human ATX, recombinant ATX were incubated at different temperatures from 40 to 70°C for 10 min. Then the remaining lysoPLD activity was measured using 14 : 0 LPC as a substrate.

Para-nitrophenyl thymidine 5′-monophosphate cleavage assay

To measure phosphodiesterase (PDE) activity towards nucleotide substrate [*para*-nitrophenyl thymidine 5′-monophosphate (*p*NP-TMP)] (*25*), recombinant ATX was mixed with *p*NP-TMP (4 mM) in assay buffer and incubated for 1 h at 37°C. Amount of *p*-nitrophenol liberated was determined by measuring optical density at 405 nm. To examine the effect of metal ions on PDE activity, recombinant ATX was pre-incubated with EDTA or EGTA for 30 min at 37°C in Mg (−) assay buffer, and the PDE activity was measured using *p*NP-TMP (4 mM) in the presence or absence of various metal ions (5 and 10 mM).

Cell migration assay

Evaluation of cell migration was performed as described previously (*26*). We used a 96-well Boyden Chamber (Neuro Probe) and polyvinylpyrrolidone free polycarbonate filter 8 μm pore (Neuro Probe) coated with fibronectin (SIGMA, Lot # 038K7555) for cell migration assay. PC-3 human prostate cancer cell was cultured in RPMI (SIGMA) supplemented with 5% FCS, antibiotics and L-glutamine. PC-3 cells (3×10^5 cells/well) and purified ATX were added to upper and lower chambers, respectively and cells were allowed to migrate for 3 h at 37°C in CO_2 incubator. After 3 h, cells on the filter were fixed by methanol and stained by Diff Quick staining. After removal of cells that did not move across the filter, cell migration was quantified by measuring optical density at 594 nm using VERSA Max microplate reader.

RT-PCR

Total RNAs from various human tissues (Ambion, Clontech, cell application) were reverse-transcribed using random primers (High Capacity cDNA Reverse Transcription Kit ABI). The PCR reaction was performed using obtained cDNAs and a set of PCR primers as follows: forward: GCCAGAGGAAGTTACCAGACC, reverse: TT GTATGAAGCCGTTTGTTGAG. The expected PCR products were 133 bp for ATXα, ATXβ and ATXγ and 121 bp for ATXδ and ATXε. These PCR products were separated by the NuSieve 3 : 1 Agarose (Lonza).

Results

Identification and cloning of human ATXδ

During the preparation of ATXβ cDNA by RT-PCR, we found a novel ATX isoform with a 12-bp deletion, which corresponded to a deletion of four amino acids located in the L2 linker region (Fig. 1). We also found several EST clones with the same deletion. We, thus, named the novel ATX isoform, ATXδ according to the names of previously identified isoforms. Other than the 12-bp deletion, the signal sequence, two somatomedin B-like domains, the catalytic domain and the nuclease-like domain were identical to ATXβ, indicating that ATXδ is catalytically active. Sequencing of 27 sub-cloned RT-PCR products from various human tissues including skeletal muscle, brain and kidney indicated that 22% of clones [six clones out of the 27 clones (6/27)] were ATXδ. Of note, 67% (18/27), 11% (3/27) and no (0/27) clones were found to be ATXβ, ATXγ and ATXα, respectively. These data indicate that ATXδ is the second most common isoform of ATX. Searching of EST database on three

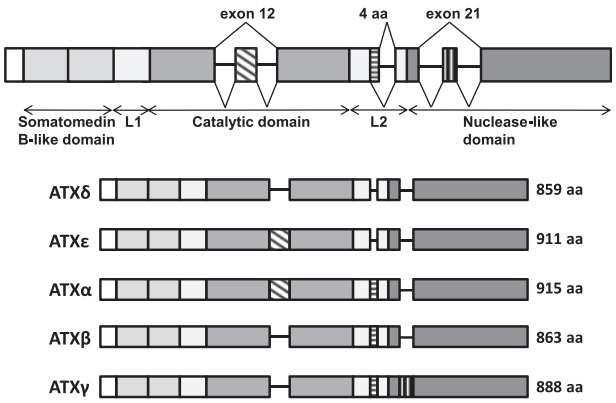

Fig. 1 Protein structure scheme of the different domains of ATX. Protein structure scheme of the domains of ATX. In ATXα, ATXβ, ATXδ and ATXε, exon 20 is spliced directly to exon 22, whereas in ATXβ, ATXγ and ATXδ exon 11 is spliced directly to exon 13. Exon 12 encodes 52 amino acids and exon 21 encodes 25 amino acids. Novel isoforms ATXδ and ATXε have four-amino acid deletions on the L2 linker (a 12-bp deletion on exon 19).

Table I. Characteristics of three slicing sites of ATX.

	Four-amino acid deletion	Fifty two-amino acid insertion	Twenty five-amino acid insertion
Location	L2 linker region Exon 19	Catalytic domain Exon 12	Nuclease domain Exon 21
Possible isoform	ATXδ, ε	ATXα, ε	ATXγ
Occurrence	17/48 (35.4%)	3/31 (9.7%)	8/55 (14.5%)

Table II. Number of EST clones with a four-amino acid deletion (exon 19), a 52-amino acid insertion (exon 12) or a 25-amino acid insertion (exon 21) in different species.

	Species						
Exon	*H. sapiens*	*M. musculus*	*R. norvegicus*	*B. taurus*	*G. gallus*	*X. laevis*	*D. rerio*
Exon 19 (−4 amino acid)	17/48 (35.4%)	5/21 (23.8%)	5/20 (25.0%)	0/25 (0%)	11/11 (100.0%)	15/15 (100.0%)	2/4 (50.0%)
Exon 12 (+52 amino acid)	3/31 (9.7%)	0/11 (0%)	0/12 (0%)	0/27 (0%)	0/6 (0%)	0/9 (0%)	0/5 (0%)
Exon 21 (+25 amino acid)	8/55 (9.1%)	1/14 (7.1%)	2/25 (8.0%)	17/22 (77.3%)	0/13 (0%)	14/17 (82.4%)	0/1 (0%)

mammalian species including *Homo sapiens*, *Mus musculus* and *Rattus norvegicus* supported the idea (Tables I and II).

Alternative splicing of ATXδ

We analysed the gene structure and nucleotide sequences around the deletion site and found that ATXδ arises from alternative splicing. The deleted sequence, gtagagccaaag in human ATXβ, encodes the four amino acids VEPK and is located at the 3′-end of the exon 19 missing in ATXδ (Fig. 2a). Two separate consensus sequences for RNA splicing (AGgta) (Fig. 2b) were found at this exon–intron boundary (*27*). It is likely that mRNA for ATXδ is produced when the first consensus site is used, and mRNA for ATXβ (or ATXα or ATXγ) is produced when the second is used (Fig. 2b). Thus, we concluded that ATXβ and ATXδ arise from alternative usage of the 5′-splicing donor sites. To see whether ATXδ is also present in other species from mammals to non-mammals, we further searched the EST database for ATXδ. We confirmed that mRNA for ATXδ was found in the database from various species including *H. sapiens*, *M. musculus*, *R. norvegicus*, *Gallus gallus*, *Xenopus laevis* and *Danio rerio*. Interestingly, we could not find any ATXδ clones in *Bos taurus* (Table II). In addition, in *G. gallus* and *X. laevis*, all the EST clones had the four-amino acid deletion (Table II), showing that the two species had no ATXβ. Alignment of the nucleotide sequence of the human, mouse, rat, chicken, Xenopus, zebrafish and bovine ATX genes around the splicing site showed that bovine ATX gene has no 5′-splicing donor sites for ATXδ (Fig. 2c), and both chicken and Xenopus ATX genes have no 5′-splicing donor sites for ATXβ. The finding that some species such as bovine (ATXβ), chicken (ATXδ) and Xenopus (ATXδ) have only one of the two ATX isoforms shows that both ATX isoforms are functionally important.

In the EST database, the isoform with the 52-amino acid insertion (exon 12) was found at a low level in human and was not detected in other species (Table II). In contrast, isoforms with the 25-amino acid insertion were common, especially, in *B. taurus* and *X. laevis* where they accounted for most of the ESTs. This suggests that ATXγ is a major isoforms in these two species.

Expression of five isoforms of ATX

We cloned ATXα and ATXγ from total RNA of A2058 and SNB-78, respectively. During the cloning of cDNA for ATXα, we found another novel isoform, designated ATXε that has both the 52-amino acid insertion in exon 12 and the four-amino acid deletion in exon 19 (Fig. 1). The five human isoforms (ATXα, ATXβ, ATXγ, ATXδ and ATXε) were transiently expressed in HEK293 cells. In the culture media, ATXβ and ATXδ were equally abundant, while ATXγ was slightly less abundant, and ATXα and ATXε were barely detectable (Fig. 3a). The PDE activities (Fig. 3b) and lysoPLD activities (Fig. 3c) of the five isoforms paralleled their abundance. In addition to their low abundances, ATXα and ATXε had significantly lower thermal stabilities than the other isoforms (Fig. 3d), so they will not be able to exist stably *in vivo*. In addition, ATXα, ATXγ and ATXε were found to be minor ATX isoforms in the EST database (Table II). Indeed, as mentioned above, we detected only 0, 3 and 0 clones for human ATXα, ATXγ and ATXε from human tissue derived total RNAs, respectively. These data showed that ATXβ and ATXδ are the major and stable isoforms, thus we gave focus on these two isoforms.

Catalytic activity of ATXδ

To characterize ATXδ catalytic activity, recombinant ATXδ was tested for its lysoPLD and PDE activities

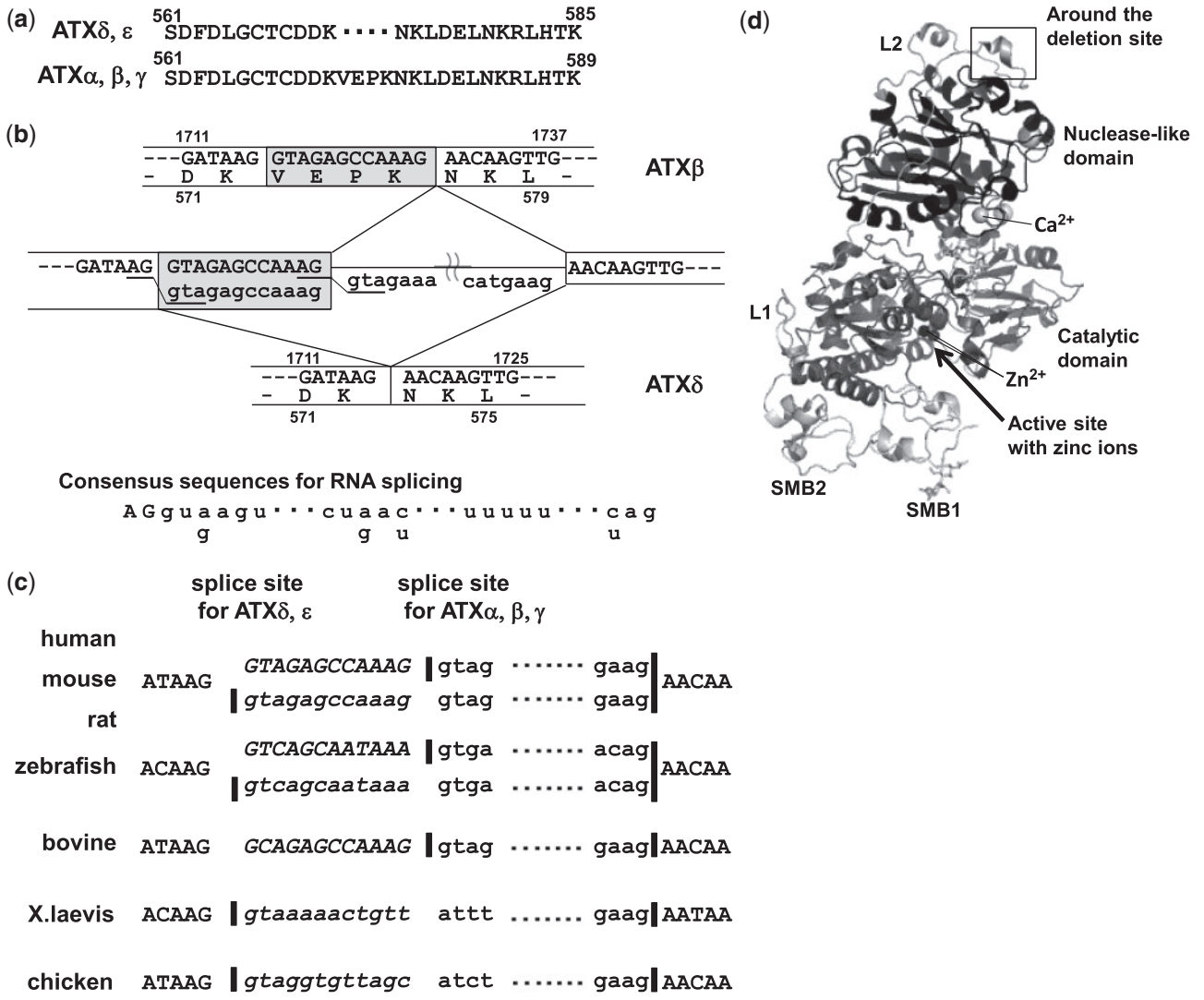

Fig. 2 Alternative splicing of ATX and a novel isoform ATXδ. (a) Amino acid sequences of ATX around the splicing site. The amino acid numbers corresponding to human ATXδ and ATXβ are shown respectively. (b) Model for alternative splicing of ATX. Two consensus 5′-splicing donor sites are located around the boundary region between exon 19 and intron 19. The two 5′-splicing donor sites are underlined. Consensus sequences for RNA splicing are shown in the lower panel. mRNAs for other isoforms of ATX (ATXα, ATXβ and ATXγ) are produced when the second 5′-splicing donor site is used; mRNAs for ATXδ and ATXε are produced when the first 5′-site is used. Upper and lower case letters indicate exons and introns, respectively. The numbers indicate nucleotide numbers corresponding to human ATXβ and ATXδ. (c) Nucleotide sequences of the human, mouse, rat, zebrafish, bovine, chicken and Xenopus ATX genes around the splicing site. Upper and lower case letters indicate exons and introns, respectively. The twelve bases (shown in italics) were found at the 5′-end of the exon–intron boundary. (d) Location of four-amino acid deletion in three-dimensional structure of mouse ATXδ. Structural figures were prepared using PyMol (DeLano Scientific).

using LPC and *p*NP-TMP as substrates, respectively. Both PDE and lysoPLD activities of ATXδ were comparable to those of ATXβ (Fig. 4a and b), showing that ATXδ is fully active. We also examined the substrate specificity of the two isoforms using LPC with various acyl groups, lysoPAF, SPC and PC. Both ATXβ and ATXδ hydrolysed various LPC species, lysoPAF and SPC, but neither hydrolysed PC (Fig. 4b). 14:0-LPC was the preferred substrate of ATXδ. The rank order was 14:0> 12:0>16:0>18:2>18:1>18:0>20:0. There were no major differences in the substrate specificity of the two isoforms. Furthermore, the two isoforms showed almost equivalent cell motility-stimulating activity toward PC-3 cancer cells (Fig. 4c).

Effect of divalent cations on PDE activity of ATXδ

The activity of ATX is significantly modified by the presence of divalent cations such as Mn^{2+} and Co^{2+} (*28*). In addition, an analysis of the crystal structure of ATX revealed that ATX has two Zn^{2+} ions in the vicinity of active site (*29*, *30*). One Zn^{2+} atom distal to the catalytic Thr^{209} coordinates one oxygen atom of the phosphate group and is critical for the activities of ATX. We, therefore, examined the role of the divalent cations on catalytic activity by incubating ATX with EDTA or EGTA. Each of the chelating agents abolished the PDE activity of both ATX isoforms in a concentration-dependent manner (Fig. 5a and b). There was no major difference in the sensitivity to these chelating agents between the two isoforms.

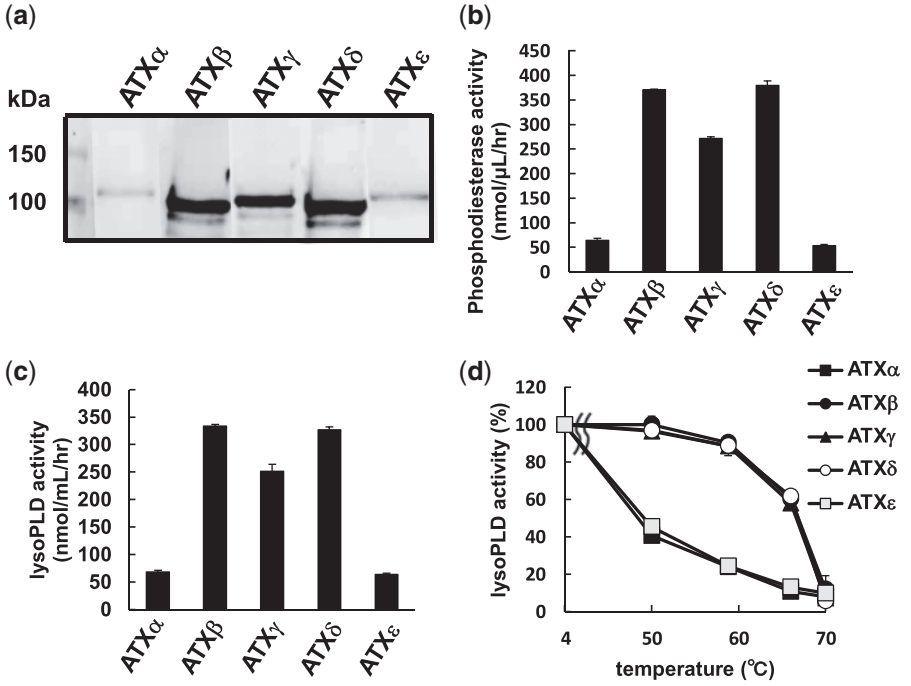

Fig. 3 Expression of five isoforms of ATX. (a) Five isoforms of ATX secreted by HEK293 cells were visualized by immunoblotting with anti-autotaxin monoclonal antibody 3D1. (b) PDE activity of human ATXα, ATXβ, ATXγ, ATXδ and ATXε using *p*NP-TMP as a substrate. (c) LysoPLD activity of human ATXα, ATXβ, ATXγ, ATXδ and ATXε using myristoyl lysophosphatidylcholine (14 : 0 LPC) as a substrate. (d) Thermal stability of human ATXα (closed squares), ATXβ (closed circles), ATXγ (closed triangles), ATXδ (open circles) and ATXε (open squares). Conditioned media from HEK293 cells transfected with human ATXα, ATXβ, ATXγ, ATXδ and ATXε cDNA was treated at different temperatures from 50 to 70°C for 10 min. All error bars represent SD ($n = 3$).

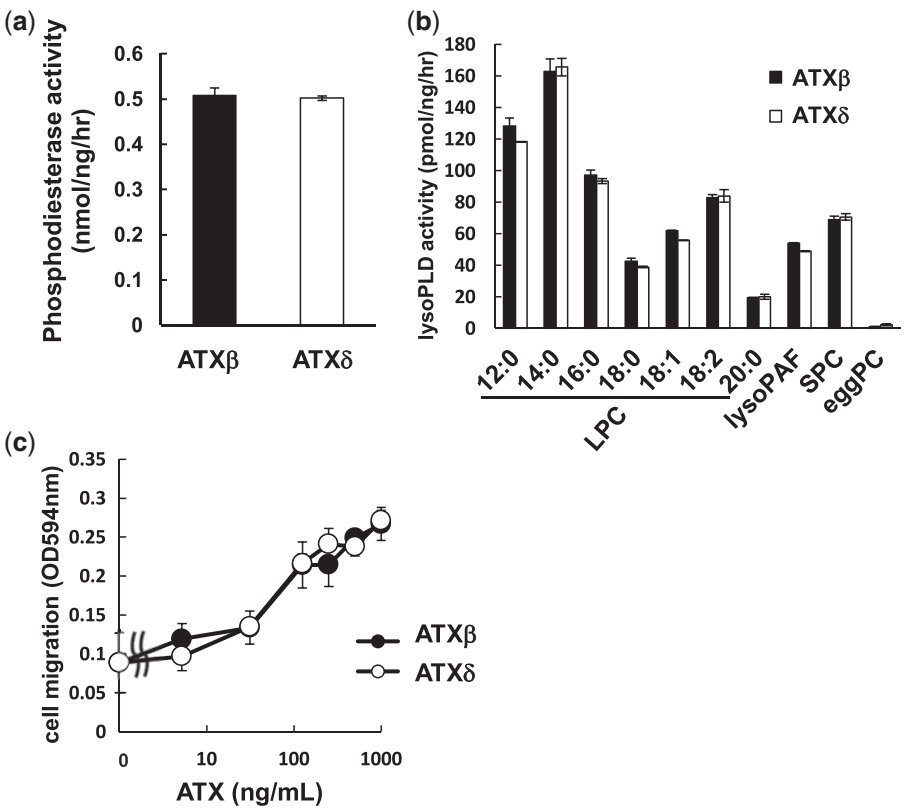

Fig. 4 Catalytic activities of ATX isoforms. (a) PDE activity of human ATXβ (closed bars) and ATXδ (open bars) using *p*NP-TMP as a substrate. (b) LysoPLD activity of human ATXβ (closed bars) and ATXδ (open bars) on LPC with various fatty acid chains (12:0, 14:0, 16:0, 18:0, 18:1, 18:2, 20:0), lysoPAF, SPC and eggPC. (c) Cell motility-stimulating activity of human ATXβ (closed circles) and ATXδ (open circles) toward PC3 prostate cancer cells in a Boyden chamber assay. All error bars represent SD ($n = 3$).

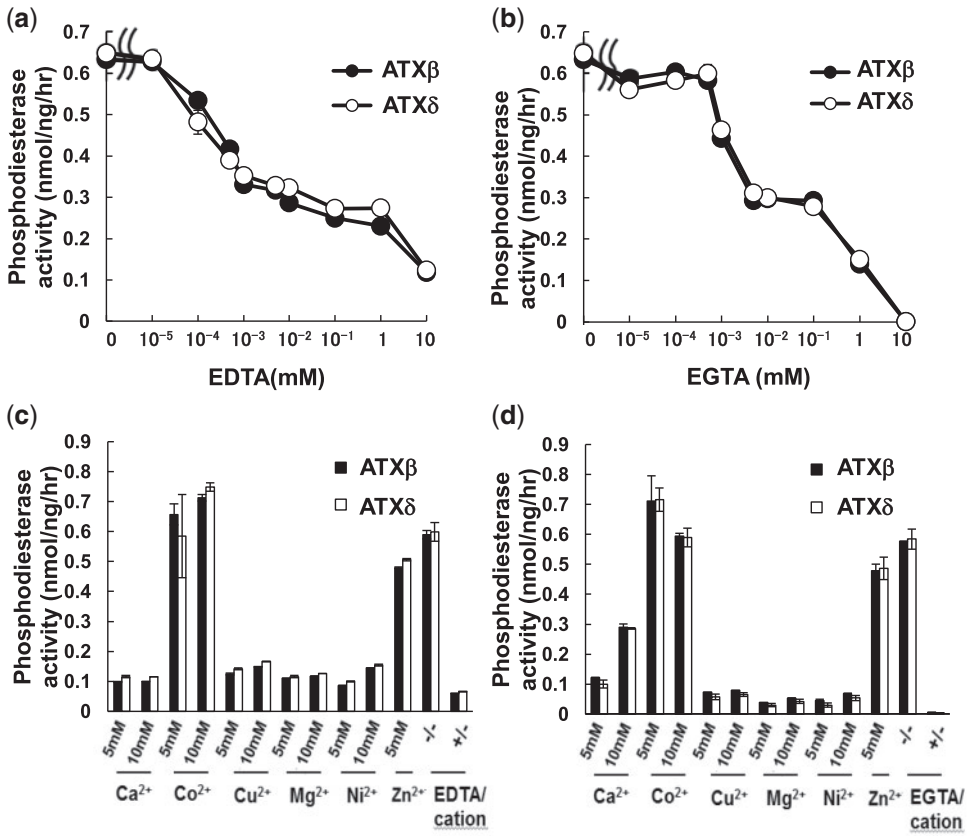

Fig. 5 Metal ion-requirement of ATX isoforms. (a and b) Effects of EDTA and EGTA on PDE activity of ATX isoforms. Recombinant human ATXβ (closed circles) and ATXδ (open circles) were incubated with *p*NP-TMP at 37°C for 1 h in the presence of varying concentrations of EDTA (a) or EGTA (b). (c and d) Effect of various divalent cations on PDE activity of ATX isoforms. Recombinant human ATXβ (closed bars) and ATXδ (open bars) were pre-incubated with EDTA (c) or EGTA (d) and various divalent cations were added back at the indicated concentration. Then, PDE activity was measured using *p*NP-TMP. All error bars represent SD ($n = 3$).

We also compared the effects of various divalent cations on PDE activity of both isoforms. The effect of added divalent cations after chelation treatment (10 mM) depended on the cation: the activities of both isoforms were restored by the addition of Co^{2+} and Zn^{2+}, but not by the addition of Mg^{2+}, Cu^{2+} nor Ni^{2+} (Fig. 5c and d). Adding Ca^{2+} to EGTA-treated ATX isoforms moderately restored ATX activity (Fig. 5d), probably because EGTA, which has a high affinity for Ca^{2+}, exchanged other divalent cations for Ca^{2+}. Again we did not observe any significant differences of divalent cation preferences between the two isoforms.

Tissue distribution of ATX isoforms

To determine the relative amounts of ATX mRNAs that have 12-bp deletions, *i.e.* the relative amounts of ATXδ and ATXε, in human tissues, RT-PCR was performed using cDNAs from total RNAs prepared from various human tissues and cell lines. To do this we designed primer pairs that span the deletion sites yielding a 133-bp product from ATXα, ATXβ and ATXγ and a 121-bp product from ATXδ and ATXε. Both bands were detected in each of the tissues examined (Fig. 6a).

Quantification of the bands indicated that the relative amount of ATX mRNAs that have 12-bp deletion (ATXδ and ATXε) was ~30% of total ATX mRNAs. But brain and retina showed relatively higher ratio of ATXα, ATXβ and ATXγ. On the other hand, small intestine and spleen had larger ratio of ATXδ and ATXε than other tissues. Both the 121 and 133-bp bands were also detected in several human cancer cell lines, in which the amount of ATXδ and ATXε was also ~30% of total ATX mRNAs.

Discussion

In this study we identified a novel splicing site in ATX that was located in exon 19 and that provided another 5′-splicing donor site. The site gave rise to a second major ATX isoform ATXδ and a minor isoform ATXε by alternative splicing. We also showed that biochemical characteristics of ATXδ were almost the same as those of ATXβ. In the crystal structures of mouse ATXδ (*29*), and rat ATXβ (*30*), the four-amino acid deletion site is on the L2 linker region connecting the catalytic and nuclease-like domains (Fig. 2d). The L2 linker wraps tightly around the nuclease-like domain and makes whole domain structurally rigid. In the crystal structures of both ATXδ and ATXβ,

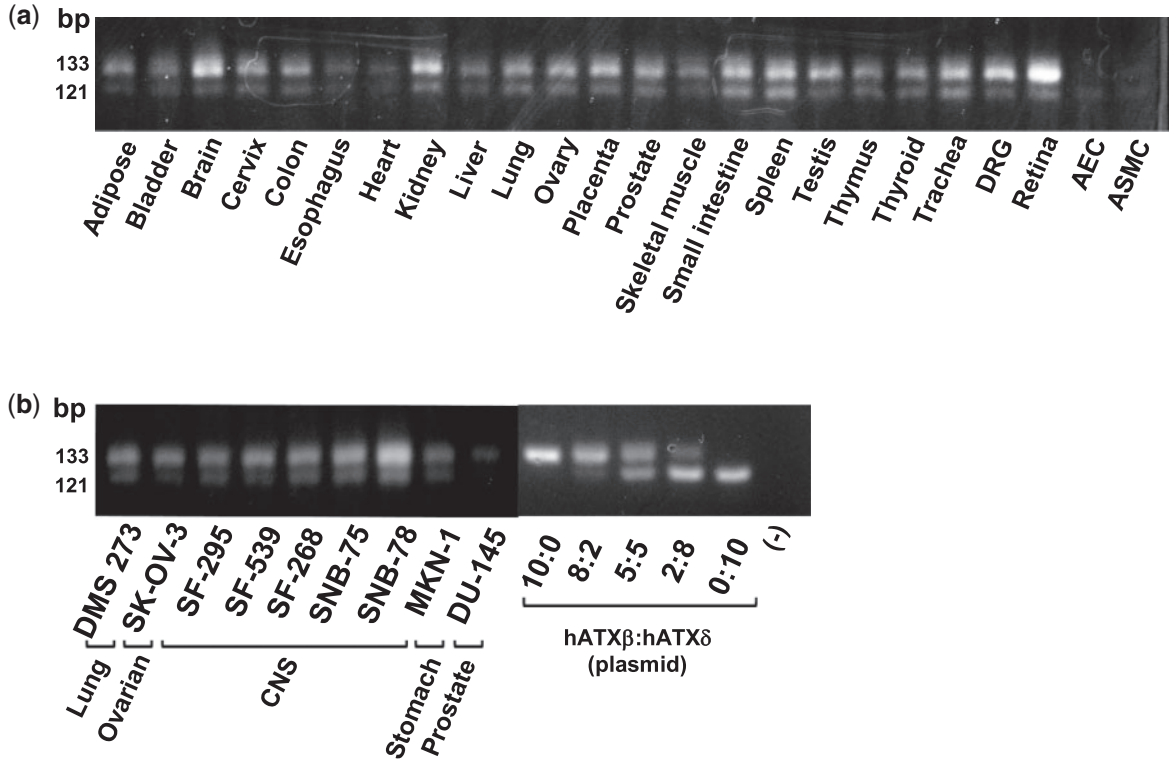

Fig. 6 Tissue distribution of ATX isoforms. (a) Tissue distribution of human ATXβ and ATXδ was examined by RT-PCR. RT-PCR was performed both in the presence or absence of reverse transcriptase. The 133-bp bands are PCR products from human ATXα, ATXβ and ATXγ and the 121-bp bands are those from human ATXδ and ATXε. DRG, dorsal root ganglion; AEC, aortic endothelial cell; ASMC, aortic smooth muscle cell; CNS, central nervous system. (b) Expression of ATXβ and ATXδ in various cancer cell lines.

the electron density around the deletion site is poorly resolved, indicating that the structures around the site are flexible and are not able to affect the whole structure, regardless of whether the four amino acids are present or absent. Importantly, the deletion site is located at the opposite side of the active centre. Thus, it is reasonable to assume that the four-amino acid deletion does not affect the structure of the active centre. This is consistent with our finding that the biochemical characteristics of ATXδ are almost the same as those of ATXβ.

Interestingly, all of the ATX ESTs that we detected in some species such as *G. gallus* and *X. laevis* had the four-amino acid deletion. Conversely, only EST clones with intact exon 19 were detected in *B. taurus*. Comparison of the genome sequences revealed that the splice donar sites for ATXδ and ATXβ are missing in *G. gallus*, *X. laevis* and *B. Taurus*, respectively, which shows that either ATXβ or ATXδ is dispensable and that ATXβ and ATXδ have redundant functions. The similar biochemical characters of the two isoforms also support this idea.

The three splicing sites in exons 12, 19 and 21 can theoretically result in eight isoforms and the five (ATXα, ATXβ, ATXγ, ATXδ and ATXε) were detected. Our present study indicated that ATXβ, ATXγ and ATXδ were expressed in relatively higher level in the culture media when expressed in HEK293 cells and that they were fully catalytically active and stable against heat treatment (Fig. 3d). By contrast, ATXα and ATXε were hardly detected in the culture media of HEK293 cells. Based on the crystal structures of mouse ATXδ and rat ATXβ, the insertion of 52 amino acids in ATXα and ATXε is located in the middle of the catalytic domain, indicating that the insertion affects the whole structure of the catalytic site. On the other hand, the insertion of 25 amino acids in ATXγ and the deletion or insertion of four amino acids may have small effects on the whole structure of the catalytic site.

Despite the similar biochemical characters of the two isoforms, their expression patterns were somewhat different in tissues and cell lines, although the average ratio of ATXβ and ATXδ was ~7 : 3. Recent studies on ATX levels in various patho-physiological conditions have indicated that the plasma ATX level is a potential indicator of the degree of liver fibrosis (*31*), the degree of pregnant toxicosis (*21*), and the progression of cancer (*19*, *20*). It is possible that the plasma ATXδ level varies under certain conditions that alter the expression pattern of ATX isoforms in a particular tissue. If so, ATXδ could be a diagnostic marker. Further measurements of ATXδ in a variety of normal and diseased human tissues are needed to test this idea.

Funding

The National Institute of Biomedical Innovation; the National Project on Protein Structural and Functional Analyses from the Ministry of Education; Precursory Research for Embryonic

Science and Technology (PRESTO, Japan Science and Technology Corporation); and Science, Sports, and Culture of Japan (to J.A.).

Conflict of interest
None declared.

References

1. Stracke, M.L., Krutzsch, H.C., Unsworth, E.J., Arestad, A., Cioce, V., Schiffmann, E., and Liotta, L.A. (1992) Identification, purification, and partial sequence analysis of autotaxin, a novel motility-stimulating protein. *J. Biol. Chem.* **267**, 2524–2529
2. Tokumura, A. (1995) A family of phospholipid autacoids: occurrence, metabolism and bioactions. *Prog. Lipid Res.* **34**, 151–184
3. Moolenaar, W.H. (1999) Bioactive lysophospholipids and their G protein-coupled receptors. *Exp. Cell Res.* **253**, 230–238
4. Contos, J.J., Fukushima, N., Weiner, J.A., Kaushal, D., and Chun, J. (2000) Requirement for the lpA1 lysophosphatidic acid receptor gene in normal suckling behavior. *Proc. Natl Acad. Sci. USA* **97**, 13384–13389
5. Ishii, I., Fukushima, N., Ye, X., and Chun, J. (2004) Lysophospholipid receptors: signaling and biology. *Annu. Rev. Biochem.* **73**, 321–354
6. Ye, X., Hama, K., Contos, J.J., Anliker, B., Inoue, A., Skinner, M.K., Suzuki, H., Amano, T., Kennedy, G., Arai, H., Aoki, J., and Chun, J. (2005) LPA3-mediated lysophosphatidic acid signalling in embryo implantation and spacing. *Nature* **435**, 104–108
7. Hama, K., Aoki, J., Inoue, A., Endo, T., Amano, T., Motoki, R., Kanai, M., Ye, X., Chun, J., Matsuki, N., Suzuki, H., Shibasaki, M., and Arai, H. (2007) Embryo spacing and implantation timing are differentially regulated by LPA3-mediated lysophosphatidic acid signaling in mice. *Biol. Reprod.* **77**, 954–959
8. Tager, A.M., LaCamera, P., Shea, B.S., Campanella, G.S., Selman, M., Zhao, Z., Polosukhin, V., Wain, J., Karimi-Shah, B.A., Kim, N.D., Hart, W.K., Pardo, A., Blackwell, T.S., Xu, Y., Chun, J., and Luster, A.D. (2008) The lysophosphatidic acid receptor LPA1 links pulmonary fibrosis to lung injury by mediating fibroblast recruitment and vascular leak. *Nat. Med.* **14**, 45–54
9. Pradere, J.P., Gonzalez, J., Klein, J., Valet, P., Gres, S., Salant, D., Bascands, J.L., Saulnier-Blache, J.S., and Schanstra, J.P. (2008) Lysophosphatidic acid and renal fibrosis. *Biochim. Biophys. Acta* **1781**, 582–587
10. Kanda, H., Newton, R., Klein, R., Morita, Y., Gunn, M.D., and Rosen, S.D. (2008) Autotaxin, an ectoenzyme that produces lysophosphatidic acid, promotes the entry of lymphocytes into secondary lymphoid organs. *Nat. Immunol.* **9**, 415–423
11. Tanaka, M., Okudaira, S., Kishi, Y., Ohkawa, R., Iseki, S., Ota, M., Noji, S., Yatomi, Y., Aoki, J., and Arai, H. (2006) Autotaxin stabilizes blood vessels and is required for embryonic vasculature by producing lysophosphatidic acid. *J. Biol. Chem.* **281**, 25822–25830
12. van Meeteren, L.A., Ruurs, P., Stortelers, C., Bouwman, P., van Rooijen, M.A., Pradere, J.P., Pettit, T.R., Wakelam, M.J., Saulnier-Blache, J.S., Mummery, C.L., Moolenaar, W.H., and Jonkers, J. (2006) Autotaxin, a secreted lysophospholipase D, is essential for blood vessel formation during development. *Mol. Cell. Biol.* **26**, 5015–5022
13. Aoki, J. (2004) Mechanisms of lysophosphatidic acid production. *Semin. Cell Dev. Biol.* **15**, 477–489
14. Aoki, J., Inoue, A., and Okudaira, S. (2008) Two pathways for lysophosphatidic acid production. *Biochim. Biophys. Acta* **1781**, 513–518
15. Tokumura, A., Harada, K., Fukuzawa, K., and Tsukatani, H. (1986) Involvement of lysophospholipase D in the production of lysophosphatidic acid in rat plasma. *Biochim. Biophys. Acta.* **875**, 31–38
16. Nakamura, K., Igarashi, K., Ide, K., Ohkawa, R., Okubo, S., Yokota, H., Masuda, A., Oshima, N., Takeuchi, T., Nangaku, M., Okudaira, S., Arai, H., Ikeda, H., Aoki, J., and Yatomi, Y. (2008) Validation of an autotaxin enzyme immunoassay in human serum samples and its application to hypoalbuminemia differentiation. *Clin. Chim. Acta* **388**, 51–58
17. Tsuda, S., Okudaira, S., Moriya-Ito, K., Shimamoto, C., Tanaka, M., Aoki, J., Arai, H., Murakami-Murofushi, K., and Kobayashi, T. (2006) Cyclic phosphatidic acid is produced by autotaxin in blood. *J. Biol. Chem.* **281**, 26081–26088
18. Ferry, G., Tellier, E., Try, A., Gres, S., Naime, I., Simon, M.F., Rodriguez, M., Boucher, J., Tack, I., Gesta, S., Chomarat, P., Dieu, M., Raes, M., Galizzi, J.P., Valet, P., Boutin, J.A., and Saulnier-Blache, J.S. (2003) Autotaxin is released from adipocytes, catalyzes lysophosphatidic acid synthesis, and activates preadipocyte proliferation. Up-regulated expression with adipocyte differentiation and obesity. *J. Biol. Chem.* **278**, 18162–18169
19. Masuda, A., Nakamura, K., Izutsu, K., Igarashi, K., Ohkawa, R., Jona, M., Higashi, K., Yokota, H., Okudaira, S., Kishimoto, T., Watanabe, T., Koike, Y., Ikeda, H., Kozai, Y., Kurokawa, M., Aoki, J., and Yatomi, Y. (2008) Serum autotaxin measurement in haematological malignancies: a promising marker for follicular lymphoma. *Br. J. Haematol.* **143**, 60–70
20. Nakai, Y., Ikeda, H., Nakamura, K., Kume, Y., Fujishiro, M., Sasahira, N., Hirano, K., Isayama, H., Tada, M., Kawabe, T., Komatsu, Y., Omata, M., Aoki, J., Koike, K., and Yatomi, Y. (2011) Specific increase in serum autotaxin activity in patients with pancreatic cancer. *Clin. Biochem.* **44**, 576–581
21. Tokumura, A., Kanaya, Y., Miyake, M., Yamano, S., Irahara, M., and Fukuzawa, K. (2002) Increased production of bioactive lysophosphatidic acid by serum lysophospholipase D in human pregnancy. *Biol. Reprod.* **67**, 1386–1392
22. Giganti, A., Rodriguez, M., Fould, B., Moulharat, N., Coge, F., Chomarat, P., Galizzi, J.P., Valet, P., Saulnier-Blache, J.S., Boutin, J.A., and Ferry, G. (2008) Murine and human autotaxin alpha, beta, and gamma isoforms - gene organization, tissue distribution, and biochemical characterization. *J. Biol. Chem.* **283**, 7776–7789
23. Tanaka, M., Kishi, Y., Takanezawa, Y., Kakehi, Y., Aoki, J., and Arai, H. (2004) Prostatic acid phosphatase degrades lysophosphatidic acid in seminal plasma. *FEBS Lett.* **571**, 197–204
24. Umezu-Goto, M., Kishi, Y., Taira, A., Hama, K., Dohmae, N., Takio, K., Yamori, T., Mills, G.B., Inoue, K., Aoki, J., and Arai, H. (2002) Autotaxin has lysophospholipase D activity leading to tumor cell growth and motility by lysophosphatidic acid production. *J. Cell. Biol.* **158**, 227–233
25. Gijsbers, R., Aoki, J., Arai, H., and Bollen, M. (2003) The hydrolysis of lysophospholipids and nucleotides

by autotaxin (NPP2) involves a single catalytic site. *FEBS Lett*. **538**, 60–64

26. Hama, K., Aoki, J., Fukaya, M., Kishi, Y., Sakai, T., Suzuki, R., Ohta, H., Yamori, T., Watanabe, M., Chun, J., and Arai, H. (2004) Lysophosphatidic acid and autotaxin stimulate cell motility of neoplastic and non-neoplastic cells through LPA1. *J. Biol. Chem*. **279**, 17634–17639
27. Warf, M.B. and Berglund, J.A. (2010) Role of RNA structure in regulating pre-mRNA splicing. *Trends Biochem. Sci*. **35**, 169–178
28. Morishige, J., Touchika, K., Tanaka, T., Satouchi, K., Fukuzawa, K., and Tokumura, A. (2007) Production of bioactive lysophosphatidic acid by lysophospholipase D in hen egg white. *Biochim. Biophys. Acta*. **1771**, 491–499
29. Nishimasu, H., Okudaira, S., Hama, K., Mihara, E., Dohmae, N., Inoue, A., Ishitani, R., Takagi, J., Aoki, J., and Nureki, O. (2011) Crystal structure of autotaxin and insight into GPCR activation by lipid mediators. *Nat. Struct. Mol. Biol*. **18**, 205–212
30. Hausmann, J., Kamtekar, S., Christodoulou, E., Day, J.E., Wu, T., Fulkerson, Z., Albers, H.M., van Meeteren, L.A., Houben, A.J., van Zeijl, L., Jansen, S., Andries, M., Hall, T., Pegg, L.E., Benson, T.E., Kasiem, M., Harlos, K., Kooi, C.W., Smyth, S.S., Ovaa, H., Bollen, M., Morris, A.J., Moolenaar, W.H., and Perrakis, A. (2011) Structural basis of substrate discrimination and integrin binding by autotaxin. *Nat. Struct. Mol. Biol*. **18**, 198–204
31. Nakagawa, H., Ikeda, H., Nakamura, K., Ohkawa, R., Masuzaki, R., Tateishi, R., Yoshida, H., Watanabe, N., Tejima, K., Kume, Y., Iwai, T., Suzuki, A., Tomiya, T., Inoue, Y., Nishikawa, T., Ohtomo, N., Tanoue, Y., Omata, M., Igarashi, K., Aoki, J., Koike, K., and Yatomi, Y. (2011) Autotaxin as a novel serum marker of liver fibrosis. *Clin. Chim. Acta* **412**, 1201–1206